

A continuous-variable quantum repeater with quantum scissors

Kaushik P. Seshadreesan¹, Hari Krovi², and Saikat Guha¹

¹*College of Optical Sciences, University of Arizona, Tucson, AZ 85721, USA*

²*Quantum Engineering and Computing Physical Sciences and Systems,
Raytheon BBN Technologies, Cambridge, MA 02138, USA*

(Dated: December 15, 2024)

The quantum scissors operation lends itself as a tool for continuous variable entanglement distillation over lossy communication channels. We show that a quantum scissors can distill a near-perfect ebit of entanglement from a two-mode squeezed vacuum state whose one share has undergone arbitrary (pure) loss, with a success probability that scales proportional to the channel transmissivity. This is akin to entanglement distillation in single-photon discrete variable entanglement distribution protocols. Invoking a multiplexing-based design for a quantum repeater scheme that was proposed for discrete variable encodings, we show a repeater scheme for CV quantum communication using quantum scissors that beats the direct-transmission rate-loss tradeoff at large distances.

I. INTRODUCTION

A quantum internet [1] of shared entanglement, and shared secret keys distributed using quantum key distribution (QKD) over long distances exemplifies the goal of quantum communications. When in place, a quantum internet would enable, e.g., unconditionally secure multiparty classical communication [2], and distributed versions of quantum computation, sensing, and other applications of quantum information processing (QIP) [3–8]. The main hurdle in way of establishing such an infrastructure is photon loss and decoherence. Quantum states, in general, and entangled quantum states that form a resource for QIP, in particular, are fragile to these phenomena. The rate at which entanglement or shared secret keys can be distributed over lossy bosonic channels is known to suffer a tradeoff with loss, which is fundamental. For example, the capacity of a pure loss channel (where the environment injects vacuum noise) for these tasks when assisted by two-way classical communication is known to be $C(\eta) = -\log_2(1 - \eta)$ [9, 10], which is $\approx 1.44\eta$ when $\eta \ll 1$, and drops exponentially with distance in fiber optic communication and inverse quadratically in free space optical communication [11].

Quantum repeaters [12, 13] have been proposed to mitigate this rate-loss tradeoff in entanglement and secret key distribution. Repeater protocols of different types [14, 15], based on matter memories [16] as well as optical memories [17, 18], have been developed for discrete-variable (DV) quantum resources such as single photon polarization or spatial dual rail qubits at rates beyond the direct transmission capacity. On the other hand, quantum continuous variables (CV), wherein the information is encoded in the continuous quadrature degrees of freedom of the electromagnetic field modes, are more naturally suited for integration with current telecommunications infrastructure, whereas the quest for quantum repeaters for CV quantum states of light remains to be conclusively settled.

It has been established that Gaussian operations alone cannot act as quantum repeaters for CV states [19, 20]. Ralph proposed a scheme based on non-deterministic

noiseless linear amplification (NLA) [21] and Gaussian CV teleportation that performs error correction [22] of CV states against the Gaussian noise arising from the action of a pure loss channel. Approximating the NLA operation using the quantum scissors [21, 23], which is a non-Gaussian operation, Dias and Ralph [24, 25] demonstrated higher logarithmic negativity and entanglement of formation of the entangled state distilled across a pure loss channel than with direct transmission. The present authors gave a lower bound on the reverse coherent information (RCI) [26–29] heralded by quantum scissors in a pure loss channel [30]. The use of NLA, both ideal [31] as well as approximate based on quantum scissors [32], was shown to increase the range of CV QKD in the presence of thermal noise. The CV error correction scheme of [22] was recently generalized to the thermal loss channel [33]. Furrer and Munro proposed a repeater scheme for continuous variable states that involves iterative use of entanglement distillation based on symmetric photon replacement and purifying distillation [34, 35] and a non-Gaussian entanglement swapping scheme that beats the repeater-less capacity at large distances [36].

In this work, we investigate a CV quantum repeater scheme with NLA based on quantum scissors [21, 23] and the non-Gaussian entanglement swap proposed in [36]. Our main contributions include the following:

- We show that the optimal exact RCI heralded by a single quantum scissors on a pure loss channel is ≈ 1 independent of the channel transmissivity η , which corresponds to heralding of a near-perfect ebit of entanglement; while the heralding success probability scales proportional to η when $\eta \ll 1$.
- Using these near-perfect ebits and the non-Gaussian entanglement swap operation, we show a mode multiplexing-based quantum repeater scheme that outperforms the direct transmission entanglement distribution rates at large distances. The multiplexed repeater differs from [36] in that it avoids iterative use of entanglement distillation, and is therefore simpler to implement.

In Sec. II, we review the multiplexed repeater scheme

discussed in [15, 16] for DV single photon sources. In Sec. III, we present an exact calculation of the RCI of the heralded state and the heralding success probability for any finite number of quantum scissors in a pure loss channel with CV entangled state input. In Sec. IV, we review the Bell state projection introduced in [36] for non-Gaussian entanglement swapping. Combining these different ingredients, in Sec. V we show a quantum repeater scheme based on quantum scissors.

II. A QUANTUM REPEATER SCHEME BASED ON MODE MULTIPLEXING

The direct transmission rate-loss tradeoff of a lossy communication channel can be circumvented by interspersing intermediate nodes that split the channel into smaller segments of manageable loss. These nodes, often called quantum repeaters, typically comprise quantum information processing elements such as a source of entanglement, entanglement distillation scheme and quantum memory. Consider a channel of transmissivity η , split into n repeater links by inserting $n - 1$ repeater nodes. The transmissivity of each repeater link is thus $t = \eta^{1/n}$. Among a few possible configurations, one possibility for a repeater link includes a single source of entanglement, followed by the loss segment, an entanglement distillation scheme and a quantum memory. In a DV single-photon-based quantum repeater scheme, the sources generate perfect dual rail Bell pairs (maximally entangled qubit pairs), one share of which are transmitted through the lossy channel segments. The transmitted photons survive the loss with a probability $p \propto t = c\eta^{1/n}$. An entanglement distillation scheme in this case simply heralds the arrival of an entangled photon through a lossy channel segment at a repeater node. At the repeater node, one local photon and one photon received through the channel are combined on a Bell-basis entangling measurement. The measurement succeeds with a probability q , accomplishing entanglement swapping across the repeater node.

The success probability p can be boosted by multiplexing each repeater link, e.g., using a large number of spectral modes from the source. For M parallel repeater links, the probability that at least one of them succeeds in distilling an ebit of entanglement is given by

$$p_M = 1 - \left(1 - c\eta^{1/n}\right)^M. \quad (1)$$

For the n -repeater link channel, where each link is M -multiplexed, the rate at which an ebit of entanglement can be distributed between the end nodes equals the probability that at least one of the M modes succeeds in each of the n links and the entanglement swaps at each of the $n - 1$ repeater nodes succeeds. It is given

(in ebits/mode) by

$$R = p_M^n q^{n-1} \leq \begin{cases} q^{n-1} \\ (Mc)^n \eta q^{n-1} \end{cases} \quad (2)$$

From the first upper bound in (2), we have $n = \log(qR_{\text{UB}})/\log q$. The two upper bounds intersect at $\eta = 1/(Mc)^n$. From the intersection, we have $n = -\log \eta / \log(Mc)$. Combining the two, we have

$$\log(qR_{\text{UB}}) = \left(\frac{\log(1/q)}{\log(Mc)}\right) \log \eta \quad (3)$$

$$\Rightarrow R_{\text{UB}} = \frac{1}{q} \eta^s, \quad s = \frac{\log(1/q)}{\log(Mc)}. \quad (4)$$

Clearly, for $M > 1/(qc)$, $s < 1$, which beats the direct transmission rate. The R_{UB} represents an upper bound on the envelope of achievable rates with the repeater scheme. The exact envelope of achievable rates with the repeater scheme was shown to be [15]

$$R = \frac{1}{q} \eta^\tau, \quad \tau = \frac{\log\left(q\left(1 - (1 - cz)^M\right)\right)}{\log z}, \quad (5)$$

where z is the unique solution of the transcendental equation

$$\begin{aligned} & \left(1 - (1 - cz)^M\right) \log\left(q\left(1 - (1 - cz)^M\right)\right) \\ &= cMz \log z (1 - cz)^{M-1}. \end{aligned} \quad (6)$$

III. REPEATER LINK BASED ON QUANTUM SCISSORS

In CV quantum communication, the source in each repeater link generates a two-mode squeezed vacuum (TMSV) state. For entanglement distillation across the lossy channel segment, in this work, we consider NLA based on quantum scissors.

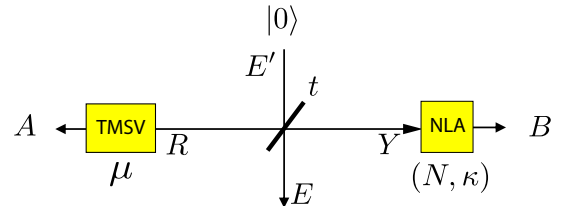


Figure 1. Repeater link: A pure loss channel of transmissivity t with TMSV state input and N -quantum scissors NLA of gain $g = \sqrt{(1 - \kappa)}/\kappa$ at the output, where κ is an intrinsic parameter in the quantum scissors.

Consider a repeater link of transmissivity t with N -quantum scissors at the output of the channel that approximate NLA of gain g , as depicted in Fig. 1. For

$N > 1$, the NLA operation consists of splitting the signal into N equal parts, where each part is acted on by a quantum scissors and recombined into one mode (c.f. [30, Fig. 1]). The TMSV state can be expressed in the Fock basis as

$$|\psi\rangle_{AR} = \sqrt{1-\chi^2} \sum_{n=0}^{\infty} \chi^n |n\rangle_A |n\rangle_R, \quad (7)$$

where $\chi = \tanh(\sinh^{-1} \sqrt{\mu})$, μ being the mean photon in each mode. By modeling the pure loss channel of transmissivity t as a beam splitter of the same transmissivity acting on the lossy mode and an environment mode that is in the vacuum state, we obtain a three-mode output state of the form

$$|\psi\rangle_{AYE} / \sqrt{1-\chi^2} \quad (8)$$

$$= \sum_{n=0}^{\infty} \chi^n \sum_{k=0}^n \sqrt{\binom{n}{k}} x^k y^{n-k} |n\rangle_A |n-k\rangle_Y |k\rangle_E \quad (9)$$

$$= \sum_{k=0}^{\infty} \sum_{n=k}^{\infty} \chi^n \sqrt{\binom{n}{k}} x^k y^{n-k} |n\rangle_A |n-k\rangle_Y |k\rangle_E \quad (10)$$

$$= \sum_{k=0}^{\infty} \sum_{m=0}^{\infty} \chi^n \sqrt{\binom{m+k}{k}} x^k y^m |m+k\rangle_A |m\rangle_Y |k\rangle_E, \quad (11)$$

where $x = \sqrt{1-t}$ and $y = \sqrt{t}$.

When NLA is successfully applied on the mode Y using N -quantum scissors, the state heralded across Alice, Bob and the environment, and the heralding success probability are given by

$$|\psi\rangle_{ABE} = \frac{c}{\sqrt{P_N}} \sum_{k=0}^{\infty} a^k \sum_{m=0}^N \frac{N!}{(N-m)!} \sqrt{\binom{m+k}{k}} b^m \times |m+k\rangle_A |m\rangle_B |k\rangle_E, \quad (12)$$

$$P_N = c^2 \sum_k a^{2k} \sum_{m=0}^N \left(\frac{N!}{(N-m)!} \right)^2 \binom{m+k}{k} b^{2m}, \quad (13)$$

where $a = \chi\sqrt{1-t}$, $b = g\chi\sqrt{t}/N$, $c = \sqrt{(1-\chi^2)\kappa^N}$, g being the NLA gain of the quantum scissors, $\kappa = 1/(1+g^2)$ being an intrinsic parameter in the quantum scissors.

The final two-mode state heralded across the NLA is obtained by tracing over the loss mode E as $\rho_{AB}^{(N)} = \sum_{u=0}^{\infty} \rho_{AB}^{(N)}(u)$, where

$$\rho_{AB}^{(N)}(u) = \sum_{m=0}^N \sum_{m'=0}^N \zeta_{m,u}^{(N)} \zeta_{m',u}^{(N)} |m+u, m\rangle \langle m'+u, m'|_{AB}, \quad (14)$$

and the coefficients $\zeta_{m,u}$ are given by

$$\zeta_{m,u}^{(N)} = ca^u b^m \frac{N!}{(N-m)!} \sqrt{\binom{m+u}{u}}. \quad (15)$$

The state $\rho_{AB}^{(N)}$ is thus

$$\rho_{AB}^{(N)} = \sum_{u=0}^{\infty} \sum_{i=0}^N \left(\zeta_{i,u}^{(N)} \right)^2 |\Phi_N(u)\rangle \langle \Phi_N(u)|_{AB} \quad (16)$$

$$|\Phi_N(u)\rangle_{AB} = \frac{\sum_{i=0}^N \left(\frac{\zeta_{i,u}^{(N)}}{\zeta_{N,u}^{(N)}} \right) |u+i, i\rangle_{AB}}{\sqrt{\sum_{i=0}^N \left(\frac{\zeta_{i,u}^{(N)}}{\zeta_{N,u}^{(N)}} \right)^2}}, \quad (17)$$

so that its entropy is given by

$$H(AB) = - \sum_{u=0}^{\infty} \left(\sum_{i=0}^N \left(\zeta_{i,u}^{(N)} \right)^2 \right) \log_2 \left(\sum_{i=0}^N \left(\zeta_{i,u}^{(N)} \right)^2 \right). \quad (18)$$

The state on system A is obtained by tracing over B as $\rho_A^{(N)} = \text{Tr}_B(\rho_{AB}^{(N)})$

$$\rho_A^{(N)} = \sum_{u=0}^{\infty} \sum_{m=0}^N \left(\zeta_{m,u}^{(N)} \right)^2 |m+u\rangle \langle m+u|_A \quad (19)$$

$$= \left(\sum_{u=0}^N \Gamma_1(u) + \sum_{u=N+1}^{\infty} \Gamma_2(u) \right) |u\rangle \langle u|_A. \quad (20)$$

where

$$\Gamma_1(u) = \sum_{\substack{\{i,j\} \geq 0, \\ i+j=u}} \left(\zeta_{i,j}^{(N)} \right)^2, \quad \Gamma_2(u) = \sum_{i=0}^N \left(\zeta_{i,u-i}^{(N)} \right)^2. \quad (21)$$

Thus, its entropy is given by

$$H(A) = - \sum_{u=0}^N \Gamma_1(u) \log_2 \Gamma_1(u) - \sum_{u=N+1}^{\infty} \Gamma_2(u) \log_2 \Gamma_2(u). \quad (22)$$

Finally, the RCI of the heralded state follows from (18) and (22) as $I_R = H(A) - H(AB)$ [26–29].

The RCI of a repeater link with a single quantum scissors, heralded upon successful operation of the scissors, is presented in Fig. 2 (a). When the heralded RCI is optimized over the mean photon number of the input TMSV state μ and the NLA gain g , the optimal value is found to be ≈ 1 , independent of the link transmissivity t , which implies heralded distillation of a near perfect ebit of entanglement at all distances. The corresponding heralding success probability is seen to scale linearly with the transmissivity t for $t \ll 1$, i.e., $R = ct$, with the proportionality constant $c \approx 5 \times 10^{-6}$. This is akin to entanglement distillation in single photon-based DV quantum communication schemes. The heralded RCI \times heralding success probability product optimized as a

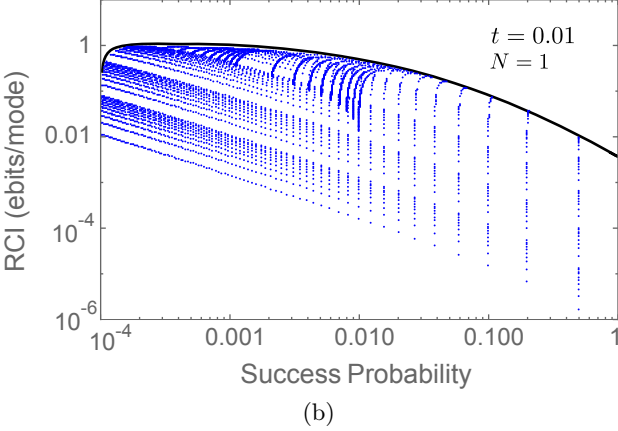
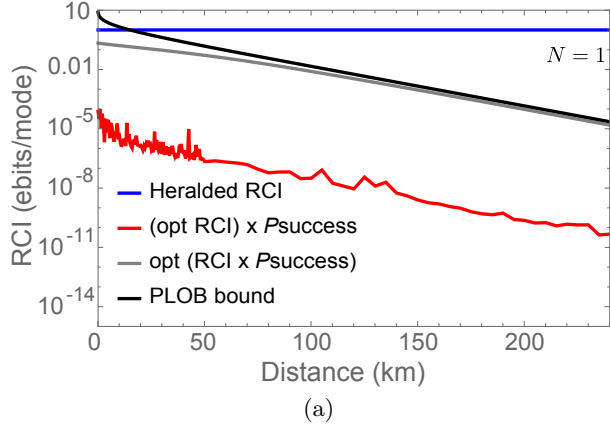


Figure 2. a) Reverse coherent information of a pure loss channel with a single quantum scissors, optimized over the TMSV input mean photon number μ and the scissors NLA gain g . (Black) is the direct transmission capacity for entanglement and secret key distillation $-\log_2(1-t)$, where $t = 10^{-0.02l}$, l being the distance of transmission. (Blue) corresponds to optimal heralded RCI at each value of distance. (Red) corresponds to the product of the optimal RCI and the corresponding heralding success probability of the scissors. (Gray) corresponds to the optimal value of the product of heralded RCI and the heralding success probability. b) A scatterplot of the heralded RCI and heralding success probability for the scheme for transmissivity $t = 0.01$ and for different choice of values of mean photon number of the TMSV and NLA gain.

whole, though, is found to be still below the repeater-less rate-loss tradeoff, which implies that the quantum scissors on average does not outperform direct transmission. Nevertheless, the fact that the quantum scissors distills a perfect ebit of entanglement every time it succeeds, lends itself compatible with the repeater scheme presented in Sec. II.

Figure 2 (b) shows a scatterplot of the heralded RCI and the heralding success probability for different values of the TMSV input mean photon number and NLA gain. The outer envelope of such a scatterplot represents the best pair of RCI and success probability achievable with a single quantum scissors at a given transmissivity, in this case $t = 0.01$.

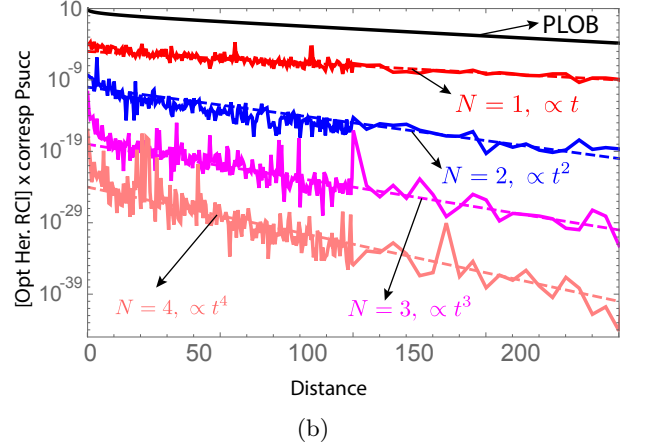
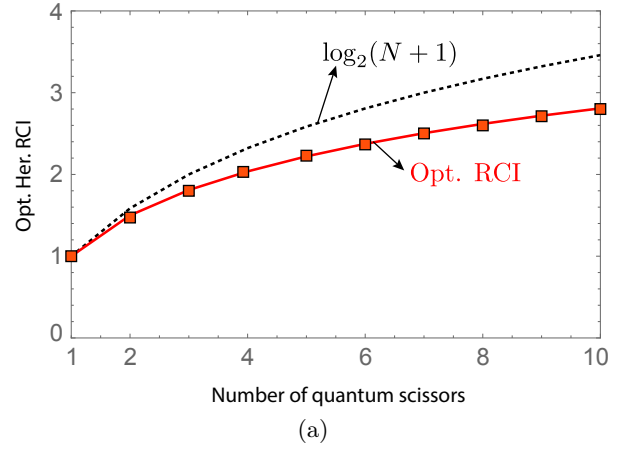


Figure 3. (a) Optimal heralded RCI as a function of the number of quantum scissors deployed in a pure loss channel (independent of channel transmissivity), where the optimization is over the TMSV input mean photon number μ and the NLA gain of the scissors g . (b) The optimal heralded RCI multiplied by the corresponding heralding success probability for $N = 1, 2, 3, 4$ quantum scissors. (The wiggles are due to numerical imprecision, but the trend is evident.)

In Fig. 3 (a), the optimal heralded RCI is plotted as a function of the number of quantum scissors N for $N = 1, 2, 3, 4$. It is seen to be below the maximum possible value of $\log_2(N+1)$, where $N+1$ is the output dimensionality of N quantum scissors. This indicates that the optimal heralded entangled states are not quite perfect “e-dits” other than for $d = 2$, i.e., with a single quantum scissors ($N = 1$). In Fig. 3 (b), the optimal heralded RCI (a constant) multiplied by the corresponding heralding success probability is plotted as a function of the transmission distance for different N . We see that this product scales proportional to t^N for channel transmissivity $t \ll 1$. Figure 4 shows that neither is the optimized product, heralded RCI \times heralding success probability, improved with increasing number of quantum scissors. These observations question the utility of higher number of quantum scissors (other than $N = 1$) in a CV quantum

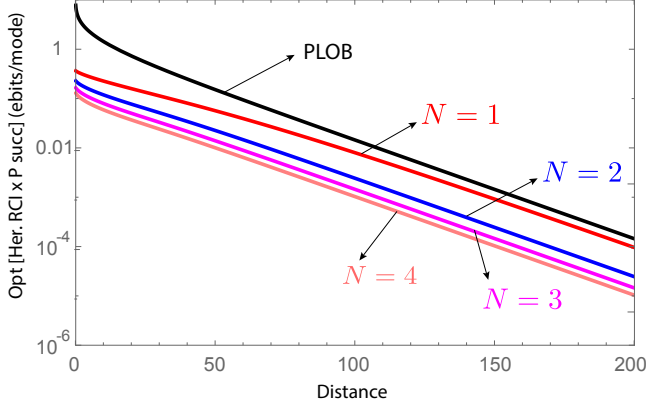


Figure 4. The optimal value of the product of heralded RCI and the heralding success probability for $N = 1, 2, 3, 4$ quantum scissors, as a function of transmission distance. The quantity is optimized over the input mean photon number μ and the NLA gain g .

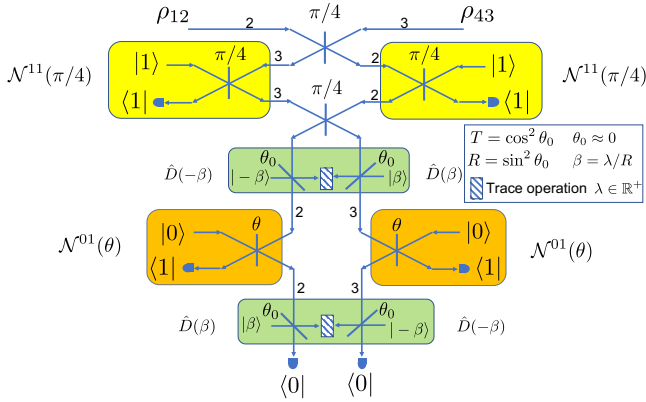


Figure 5. A Non-Gaussian entanglement swap operation based on Fock state filtering, displacement operations, photon subtraction and vacuum projection. See Appendix for more details.

repeater scheme.

IV. NON-GAUSSIAN ENTANGLEMENT SWAPPING

Since the entanglement distilled in each repeater link with a single quantum scissors is nearly a perfect ebit, the heralded state, to first approximation, is a pure state of the form

$$|\psi\rangle_{A_1 B_1} = (|0\rangle_{A_1} |0\rangle_{B_1} + \xi |1\rangle_{A_1} |1\rangle_{B_1}) / \sqrt{1 + \xi^2}. \quad (23)$$

At a repeater node, the entanglement in two such states $|\psi\rangle_{A_1 B_1}$ and $|\psi\rangle_{A_2 B_2}$ can be swapped by a Bell state projection of the form $\hat{\Pi} = |\phi\rangle\langle\phi|_{B_1 A_2}$, where $|\phi\rangle_{B_1 A_2} = (\xi |0\rangle_{B_1} |0\rangle_{A_2} + |1\rangle_{B_1} |1\rangle_{A_2}) / \sqrt{1 + \xi^2}$. Such a Bell state projection can be implemented by Fock state filtering [34]

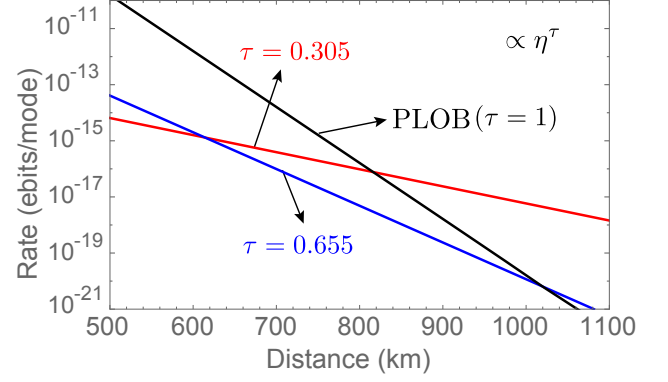


Figure 6. Entanglement distribution rates achieved by the multiplexed repeater scheme as a function of transmission distance over an optical fiber of 0.2 dB/km loss. The different τ parameters correspond to different multiplexing and represent the envelope of rates achievable with the chosen level of multiplexing when the number of repeater nodes is varied.

and a sequence of displacement operations, photon subtraction and vacuum projection [36] as shown in Fig. 5. (See Appendix for more details about this projection.) The success probability of this projection is found to be

$$q = \frac{\xi^2}{1 + \xi^2} \frac{\cos^4 \theta (\sin^2 \theta)^\xi}{16}, \quad (24)$$

where $\sin^2 \theta$ is the reflectivity of the beam splitter used for photon subtraction in Fig. 5.

V. IDEAL MULTIPLEXED REPEATER BASED ON QUANTUM SCISSORS

With $c = 5 \times 10^{-6}$ and q as given in (24) and optimized over θ (the optimum value is found to be ≈ 0.00463), we can now apply the multiplexed repeater rate formula from (5) for the CV repeater scheme with quantum scissors. Figure 7 shows a schematic of the repeater scheme. With $M \approx 10^9$, the scheme can attain an entanglement distribution rate that scales as η^τ , where $\tau = 0.655$, which is found to beat the direct transmission rate at ≈ 1000 km transmission distance over an optical fiber of 0.2 dB/km loss. Likewise, with $M \approx 10^{13}$, the scheme can attain a rate exponent $\tau = 0.305$, which beats the direct transmission rate at ≈ 800 kms. Figure 6 shows these rates in comparison to the direct transmission rate. The line corresponding to each value of τ represents the envelope of rates that can be attained with different number of repeater nodes along the channel with the corresponding M -multiplexing of each repeater link. For each distance there exists an optimal number of repeater nodes whose rate would match the rate η^τ .

The simplicity of the above calculation of the repeater performance was a consequence of operating the quantum scissors at the optimal parameter values which yield

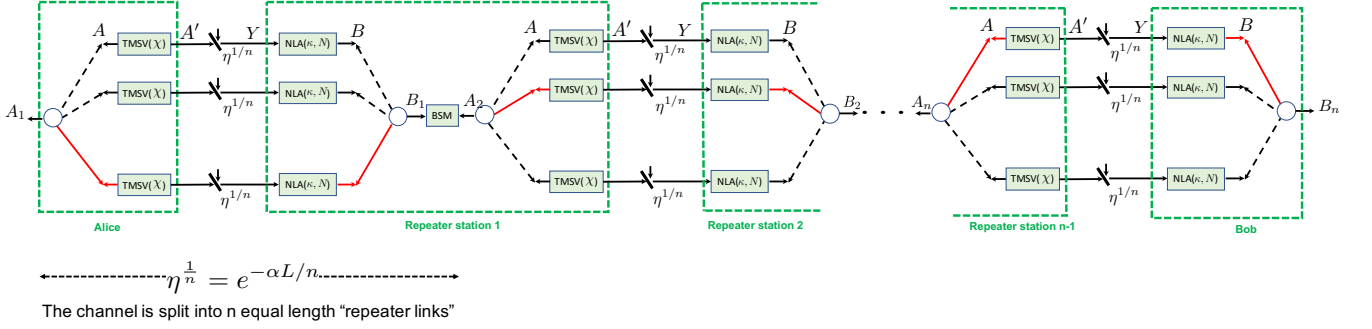


Figure 7. An illustration of the multiplexed CV quantum repeater scheme.

a constant RCI of ≈ 1 at all transmissivities every time the scissors succeeds. The corresponding success probability scaled proportional to the transmissivity, which was boosted using multiplexing. However, this is not necessarily the optimal operation of the repeater scheme. The quantum scissors could be operated at a different set of parameter values, which, e.g., do not yield a perfect ebit of entanglement, but herald entanglement at a higher success probability. The rate supported by the multiplexed repeater scheme for such an operation is not as easy to calculate. It would involve determining an iterative sequence of states heralded after different number of entanglements swaps, the corresponding success probabilities and swapping success probability. Yet, it could lead to a higher repeater-enhanced entanglement distribution rates, which constitutes a task for future work.

In summary, we discussed a multiplexing-based repeater scheme using quantum scissors and a non-Gaussian entanglement swap operation for CV quantum communication over a pure loss bosonic channel. The scheme is similar in spirit to its DV counterpart [15]. We justified this proposal by showing that the quantum scissors can be optimized to distill nearly perfect ebits

independent of the channel transmissivity, with a success probability that scales linearly with transmissivity, which is similar to the case of single-photon-based DV entanglement distillation schemes. We showed that the repeater scheme can beat the direct transmission entanglement distillation rate, e.g., at a distance ≈ 1000 km with a multiplexing $M \approx 10^9$.

ACKNOWLEDGMENTS

This work was supported by the Office of Naval Research program Communications and Networking with Quantum Operationally-Secure Technology for Maritime Deployment (CONQUEST), awarded under Raytheon BBN Technologies prime contract number N00014-16-C-2069, and a subcontract to University of Arizona. This document does not contain technology or technical data controlled under either the U.S. International Traffic in Arms Regulations or the U.S. Export Administration Regulations.

-
- [1] H. J. Kimble. The quantum internet. *Nature*, 453:1023, June 2008.
 - [2] Valerio Scarani, Helle Bechmann-Pasquinucci, Nicolas J. Cerf, Miloslav Dušek, Norbert Lütkenhaus, and Momtchil Peev. The security of practical quantum key distribution. *Rev. Mod. Phys.*, 81:1301–1350, Sep 2009.
 - [3] Timothy J. Proctor, Paul A. Knott, and Jacob A. Dunningham. Multiparameter estimation in networked quantum sensors. *Phys. Rev. Lett.*, 120:080501, Feb 2018.
 - [4] Wenchao Ge, Kurt Jacobs, Zachary Eldredge, Alexey V. Gorshkov, and Michael Foss-Feig. Distributed quantum metrology with linear networks and separable inputs. *Phys. Rev. Lett.*, 121:043604, Jul 2018.
 - [5] Quntao Zhuang, Zheshen Zhang, and Jeffrey H. Shapiro. Distributed quantum sensing using continuous-variable multipartite entanglement. *Phys. Rev. A*, 97:032329, Mar 2018.
 - [6] R. Van Meter and S. J. Devitt. The path to scalable distributed quantum computing. *Computer*, 49(9):31–42, Sept 2016.
 - [7] Vincent Danos, Ellie D’Hondt, Elham Kashefi, and Prakash Panangaden. Distributed measurement-based quantum computation. *Electronic Notes in Theoretical Computer Science*, 170:73 – 94, 2007. Proceedings of the 3rd International Workshop on Quantum Programming Languages (QPL 2005).
 - [8] Harry Buhrman and Hein Röhrig. Distributed quantum computing. In Branislav Rován and Peter Vojtáš, editors, *Mathematical Foundations of Computer Science 2003*, pages 1–20, Berlin, Heidelberg, 2003. Springer Berlin Heidelberg.
 - [9] Stefano Pirandola, Riccardo Laurenza, Carlo Ottaviani, and Leonardo Banchi. Fundamental limits of repeaterless quantum communications. *Nature Communications*, 8:15043, April 2017.
 - [10] M. M. Wilde, M. Tomamichel, and M. Berta. Con-

- verse bounds for private communication over quantum channels. *IEEE Transactions on Information Theory*, 63(3):1792–1817, March 2017.
- [11] Masahiro Takeoka, Saikat Guha, and Mark M. Wilde. Fundamental rate-loss tradeoff for optical quantum key distribution. *Nature Communications*, 5:1–13, 2014.
- [12] William J. Munro, Koji Azuma, Kiyoshi Tamaki, and Kae Nemoto. Inside Quantum Repeaters. *IEEE Journal of Selected Topics in Quantum Electronics*, 21(3), 2015.
- [13] H.-J. Briegel, W. Dür, J. I. Cirac, and P. Zoller. Quantum repeaters: The role of imperfect local operations in quantum communication. *Phys. Rev. Lett.*, 81:5932–5935, Dec 1998.
- [14] Sreraman Muralidharan, Linshu Li, Jungsang Kim, Norbert Lütkenhaus, Mikhail D. Lukin, and Liang Jiang. Optimal architectures for long distance quantum communication. *Scientific Reports*, 6:20463, February 2016.
- [15] Saikat Guha, Hari Krovi, Christopher A. Fuchs, Zachary Dutton, Joshua A. Slater, Christoph Simon, and Wolfgang Tittel. Rate-loss analysis of an efficient quantum repeater architecture. *Phys. Rev. A*, 92:022357, Aug 2015.
- [16] Neil Sinclair, Erhan Saglamyurek, Hassan Mallahzadeh, Joshua A. Slater, Mathew George, Raimund Ricken, Morgan P. Hedges, Daniel Oblak, Christoph Simon, Wolfgang Sohler, and Wolfgang Tittel. Spectral multiplexing for scalable quantum photonics using an atomic frequency comb quantum memory and feed-forward control. *Phys. Rev. Lett.*, 113:053603, Jul 2014.
- [17] Mihir Pant, Hari Krovi, Dirk Englund, and Saikat Guha. Rate-distance tradeoff and resource costs for all-optical quantum repeaters. *Phys. Rev. A*, 95:012304, Jan 2017.
- [18] Koji Azuma, Kiyoshi Tamaki, and Hoi-Kwong Lo. All-photon quantum repeaters. *Nature Communications*, 6:6787, April 2015.
- [19] Ryo Namiki, Oleg Gittsovich, Saikat Guha, and Norbert Lütkenhaus. Gaussian-only regenerative stations cannot act as quantum repeaters. *Phys. Rev. A*, 90:062316, Dec 2014.
- [20] Jason Hoelscher-Obermaier and Peter van Loock. Optimal gaussian entanglement swapping. *Phys. Rev. A*, 83:012319, Jan 2011.
- [21] T. C. Ralph and A. P. Lund. Nondeterministic noiseless linear amplification of quantum systems. *AIP Conference Proceedings*, 1110(1):155–160, 2009.
- [22] T. C. Ralph. Quantum error correction of continuous-variable states against Gaussian noise. *Physical Review A - Atomic, Molecular, and Optical Physics*, 84(2):1–4, 2011.
- [23] David T. Pegg, Lee S. Phillips, and Stephen M. Barnett. Optical state truncation by projection synthesis. *Phys. Rev. Lett.*, 81:1604–1606, Aug 1998.
- [24] Josephine Dias and T. C. Ralph. Quantum repeaters using continuous-variable teleportation. *Physical Review A*, 95(2):1–10, 2017.
- [25] Josephine Dias and T. C. Ralph. Quantum error correction of continuous-variable states with realistic resources. *Physical Review A*, 97(3):1–8, 2018.
- [26] Igor Devetak and Andreas Winter. Distillation of secret key and entanglement from quantum states. *Proceedings of the Royal Society of London A: Mathematical, Physical and Engineering Sciences*, 461(2053):207–235, 2005.
- [27] Frédéric Grosshans. Collective attacks and unconditional security in continuous variable quantum key distribution. *Phys. Rev. Lett.*, 94:020504, Jan 2005.
- [28] Igor Devetak, Marius Junge, Christopher King, and Mary Beth Ruskai. Multiplicativity of completely bounded p-norms implies a new additivity result. *Communications in Mathematical Physics*, 266(1):37–63, Aug 2006.
- [29] Raúl García-Patrón, Stefano Pirandola, Seth Lloyd, and Jeffrey H. Shapiro. Reverse coherent information. *Phys. Rev. Lett.*, 102:210501, May 2009.
- [30] Kaushik P. Seshadreesan, Hari Krovi, and Saikat Guha. Continuous-variable entanglement distillation over a pure loss channel with quantum scissors. submitted to arXiv.
- [31] Rémi Blandino, Anthony Leverrier, Marco Barbieri, Jean Etesse, Philippe Grangier, and Rosa Tualle-Brouiri. Improving the maximum transmission distance of continuous-variable quantum key distribution using a noiseless amplifier. *Phys. Rev. A*, 86:012327, Jul 2012.
- [32] Masoud Ghalaii, Carlo Ottaviani, Rupesh Kumar, Stefano Pirandola, and Mohsen Razavi. Long-distance continuous-variable quantum key distribution with quantum scissors, 2018. arXiv:1808.01617v1.
- [33] Spyros Tserkis, Josephine Dias, and Timothy C. Ralph. Simulation of Gaussian channels via teleportation and error correction of Gaussian states, 2018. arXiv:1803.03516v2.
- [34] Jaromír Fiurášek. Distillation and purification of symmetric entangled gaussian states. *Phys. Rev. A*, 82:042331, Oct 2010.
- [35] Daniel E. Browne, Jens Eisert, Stefan Scheel, and Martin B. Plenio. Driving non-gaussian to gaussian states with linear optics. *Phys. Rev. A*, 67:062320, Jun 2003.
- [36] Fabian Furrer and William J. Munro. Repeaters for continuous-variable quantum communication. *Phys. Rev. A*, 98:032335, Sep 2018.

Appendix: Non-Gaussian Entanglement Swap

A beam splitter of transmissivity $T = \cos^2 \theta$ acting on modes i and j can be described by the unitary operator:

$$U_{ij}(\theta) = \exp\left(-\theta\left(\hat{a}_i^\dagger \hat{a}_j - \hat{a}_j^\dagger \hat{a}_i\right)\right), \quad (\text{A.1})$$

that transforms the mode operators as

$$\begin{pmatrix} \hat{a}_i \\ \hat{a}_j \end{pmatrix} \rightarrow U_{ij}(\theta)^\dagger \begin{pmatrix} \hat{a}_i \\ \hat{a}_j \end{pmatrix} U_{ij}(\theta) \quad (\text{A.2})$$

$$= \begin{pmatrix} \cos \theta & \sin \theta \\ -\sin \theta & \cos \theta \end{pmatrix} \begin{pmatrix} \hat{a}_i \\ \hat{a}_j \end{pmatrix}. \quad (\text{A.3})$$

It's action on a Fock state input $|n\rangle_i \otimes |0\rangle_j$ is given by

$$U_{ij}(\theta) |n\rangle_i |0\rangle_j = \sum_{k=0}^n \sqrt{\binom{n}{k}} (\cos^2 \theta)^{k/2} (\sin^2 \theta)^{(n-k)/2} |k\rangle_i |n-k\rangle_j. \quad (\text{A.4})$$

Proposition 1. Consider the channel comprising of mixing an input mode i with a mode j in the Fock state $|1\rangle_j$ on a beam splitter $U_{ij}(\theta)$, followed by a projective measurement $\langle 1|_i$ in mode i . Let us denote this non-trace-preserving map as $\mathcal{N}_{i \rightarrow j}^{11}(\theta)$. It can be written as

$$\mathcal{N}_{i \rightarrow j}^{11}(\theta) = \left(-\sin \theta + \cos \theta \frac{d}{d\theta} \right) (\sin \theta)^{\hat{n}_{ij}}, \quad (\text{A.5})$$

where we use the notation $\hat{n}_{ij} |n\rangle_i = |n\rangle_j$ to denote input to output transformation.

Proof. We have

$$U_{ij}(\theta) |n\rangle_i |1\rangle_j = U_{ij}(\theta) \hat{a}_j^\dagger |n\rangle_i |0\rangle_j \quad (\text{A.6})$$

$$= \left(-\sin \theta \hat{a}_i^\dagger + \cos \theta \hat{a}_j^\dagger \right) U_{ij}(\theta) |n\rangle_i |0\rangle_j \quad (\text{A.7})$$

This implies

$$\langle 1|_i U_{ij}(\theta) |n\rangle_i |1\rangle_j = \langle 0|_i \hat{a}_i \left(-\sin \theta \hat{a}_i^\dagger + \cos \theta \hat{a}_j^\dagger \right) U_{ij}(\theta) |n\rangle_i |0\rangle_j \quad (\text{A.8})$$

$$= -\sin \theta \langle 0|_i \hat{a}_i \hat{a}_i^\dagger U_{ij}(\theta) |n\rangle_i |0\rangle_j + \cos \theta \langle 0|_i \hat{a}_i \hat{a}_j^\dagger U_{ij}(\theta) |n\rangle_i |0\rangle_j \quad (\text{A.9})$$

$$= -\sin \theta \langle 0|_i \left(1 + \hat{a}_i^\dagger \hat{a}_i \right) U_{ij}(\theta) |n\rangle_i |0\rangle_j + \cos \theta \langle 0|_i \hat{a}_i \hat{a}_j^\dagger U_{ij}(\theta) |n\rangle_i |0\rangle_j \quad (\text{A.10})$$

$$= -\sin \theta \langle 0|_i U_{ij}(\theta) |n\rangle_i |0\rangle_j + \cos \theta \langle 0|_i \hat{a}_i \hat{a}_j^\dagger U_{ij}(\theta) |n\rangle_i |0\rangle_j \quad (\text{A.11})$$

$$= -\sin^{n+1} \theta |n\rangle_j + n \cos^2 \theta \sin^{n-1} \theta |n\rangle_j \quad (\text{A.12})$$

$$= \left(-\sin \theta + \cos \theta \frac{d}{d\theta} \right) \sin^n \theta |n\rangle_j, \quad (\text{A.13})$$

which implies, for a general state $|\psi\rangle_i = \sum_n c_n |n\rangle_i$, the action of the channel is as given in (A.5). \square

Proposition 2. Consider the channel comprising of mixing an input mode i with a mode j in the Fock state $|0\rangle_j$ on a beam splitter $U_{ij}(\theta)$, followed by a projective measurement $\langle 1|_i$ in the mode i . Let us denote this non-trace-preserving map as $\mathcal{N}_{i \rightarrow j}^{01}(\theta)$. It can be written as

$$\mathcal{N}_{i \rightarrow j}^{01}(\theta) = \cos \theta (\sin \theta)^{\hat{n}_{ij}} \hat{a}_j \quad (\text{A.14})$$

where we use the notation $\hat{n}_{ij} |n\rangle_i = |n\rangle_j$ to denote the input to output transformation.

Proof. From (A.4), we have

$$\begin{aligned} \langle 1|_i U_{ij}(\theta) |n\rangle_i |0\rangle_j &= \sqrt{n} \cos \theta \sin^{n-1} \theta |n-1\rangle_j \\ &= \hat{a}_j \cos \theta \sin^{n-1} \theta |n\rangle_j \\ &= \cos \theta (\sin \theta)^{\hat{n}_{ij}} \hat{a}_j |n\rangle_j \end{aligned}$$

which implies, for a general state $|\psi\rangle_i = \sum_n c_n |n\rangle_i$, the action of the channel is as given in (A.14). \square

Remark 3. The displacement operation $\hat{D}_i(\lambda)$ on a mode i can be implemented using a beam splitter $U_{ij}(\theta)$ with the mode j in the coherent state $|\lambda/\sin^2\theta\rangle_j$.

Proposition 4. Consider the measurement depicted in Fig. 5. The projection implemented by the measurement scheme on modes 2 and 3 is given by

$$\hat{F}_{23} = -\cos^2\theta (\sin^2\theta)^{\lambda^2} \left(\frac{\lambda^2}{2} |0\rangle_2 |0\rangle_3 + \frac{1}{4} |1\rangle_2 |1\rangle_3 \right),$$

where θ is related to the transmissivity of the photon subtraction beam splitters and λ is the amplitude of the displacement stages.

Proof. The measurement scheme depicted in Fig. 5 implements the projection

$$\langle 0, 0 |_{23} \hat{D}_3(-\lambda) \mathcal{N}_{3 \rightarrow 3''}^{01}(\theta)_{\theta \rightarrow 0} \hat{D}_3(\lambda) \hat{D}_2(\lambda) \mathcal{N}_{2 \rightarrow 2''}^{01}(\theta)_{\theta \rightarrow 0} \hat{D}_2(-\lambda) U_{23}^\dagger(\pi/4) \mathcal{N}_{2 \rightarrow 2'}^{11}(\pi/4) \mathcal{N}_{3 \rightarrow 3'}^{11}(\pi/4) U_{23}(\pi/4), \quad (\text{A.15})$$

where for brevity of notation the primes on the output modes of individual elements in the transformation are suppressed ahead of the subsequent elements, and $\lambda \in \mathbb{R}^+$.

From, (A.14), we have

$$\begin{aligned} \langle 0 |_2 \hat{D}_2(\lambda) (\mathcal{N}_{2 \rightarrow 2''}^{01}(\theta)) \hat{D}_2(-\lambda) &= \langle 0 |_2 \hat{D}_2(\lambda) \cos\theta (\sin\theta)^{\hat{n}_2} \hat{a}_2 \hat{D}_2(-\lambda) \\ &= \cos\theta (\sin\theta)^{\lambda^2} \langle -\lambda |_2 \hat{a}_2 \hat{D}_2(-\lambda) \\ &= \cos\theta (\sin\theta)^{\lambda^2} \langle 0 |_2 \hat{D}_2(\lambda) \hat{a}_2 \hat{D}_2(-\lambda) \\ &= \cos\theta (\sin\theta)^{\lambda^2} \langle 0 |_2 (\hat{a}_2 - \lambda) \\ &= \cos\theta (\sin\theta)^{\lambda^2} (\langle 1 |_2 - \lambda \langle 0 |_2). \end{aligned}$$

Likewise,

$$\langle 0 |_3 \hat{D}_3(-\lambda) (\mathcal{N}_{3 \rightarrow 3''}^{01}(\theta)) \hat{D}_3(\lambda) = \cos\theta (\sin\theta)^{\lambda^2} (\langle 1 |_3 + \lambda \langle 0 |_3).$$

From (A.5),

$$\mathcal{N}^{11}(\pi/4) |n\rangle = -\left(\frac{1}{\sqrt{2}}\right)^{n+1} + n \left(\frac{1}{\sqrt{2}}\right)^2 \left(\frac{1}{\sqrt{2}}\right)^{n-1} |n\rangle \quad (\text{A.16})$$

$$= \frac{(n-1)}{(\sqrt{2})^{n+1}} |n\rangle. \quad (\text{A.17})$$

Therefore, we have

$$\mathcal{N}^{11}(\pi/4) = \frac{(\hat{n} - 1)}{(\sqrt{2})^{\hat{n}+1}}.$$

Thus, the projection in (A.15) can be written as

$$\begin{aligned} \hat{F}_{23}^\dagger &= \cos^2\theta (\sin^2\theta)^{\lambda^2} (\langle 1 |_3 + \lambda \langle 0 |_3) (\langle 1 |_2 - \lambda \langle 0 |_2) U_{23}^\dagger(\pi/4) \frac{(\hat{n}_2 - 1)}{(\sqrt{2})^{\hat{n}_2+1}} \frac{(\hat{n}_3 - 1)}{(\sqrt{2})^{\hat{n}_3+1}} U_{23}(\pi/4) \\ &= \cos^2\theta (\sin^2\theta)^{\lambda^2} (\langle 1 |_3 + \lambda \langle 0 |_3) (\langle 1 |_2 - \lambda \langle 0 |_2) U_{23}^\dagger(\pi/4) (\hat{n}_2 - 1) \frac{1}{(\sqrt{2})^{\hat{n}_2+\hat{n}_3+2}} (\hat{n}_3 - 1) U_{23}(\pi/4) \\ &= \cos^2\theta (\sin^2\theta)^{\lambda^2} (\langle 1 |_3 + \lambda \langle 0 |_3) (\langle 1 |_2 - \lambda \langle 0 |_2) \\ &\quad \times U_{23}^\dagger(\pi/4) (\hat{n}_2 - 1) U_{23}(\pi/4) U_{23}^\dagger(\pi/4) \frac{1}{(\sqrt{2})^{\hat{n}_2+\hat{n}_3+2}} U_{23}(\pi/4) U_{23}^\dagger(\pi/4) (\hat{n}_3 - 1) U_{23}(\pi/4). \end{aligned}$$

From (A.3), we have

$$U_{23}^\dagger(\pi/4)(\hat{n}_3 - 1)U_{23}(\pi/4) = \frac{(\hat{a}_2^\dagger - \hat{a}_3^\dagger)(\hat{a}_2 - \hat{a}_3)}{2} - 1$$

$$U_{23}^\dagger(\pi/4)(\hat{n}_2 - 1)U_{23}(\pi/4) = \frac{(\hat{a}_2^\dagger + \hat{a}_3^\dagger)(\hat{a}_2 + \hat{a}_3)}{2} - 1.$$

Thus, we have

$$\hat{F}_{23}^\dagger = \cos^2 \theta (\sin^2 \theta)^{\lambda^2} (\langle 1|_3 + \lambda \langle 0|_3) (\langle 1|_2 - \lambda \langle 0|_2) \left(\frac{(\hat{a}_2^\dagger + \hat{a}_3^\dagger)(\hat{a}_2 + \hat{a}_3)}{2} - 1 \right) \frac{1}{(\sqrt{2})^{\hat{n}_3 + \hat{n}_2 + 2}} \left(\frac{(\hat{a}_2^\dagger - \hat{a}_3^\dagger)(\hat{a}_2 - \hat{a}_3)}{2} - 1 \right).$$

The projector can be written in the ket form as

$$\begin{aligned} \hat{F}_{23} &= \cos^2 \theta (\sin^2 \theta)^{\lambda^2} \left(\frac{(\hat{a}_2^\dagger + \hat{a}_3^\dagger)(\hat{a}_2 + \hat{a}_3)}{2} - 1 \right) \frac{1}{(\sqrt{2})^{\hat{n}_3 + \hat{n}_2 + 2}} \left(\frac{(\hat{a}_2^\dagger - \hat{a}_3^\dagger)(\hat{a}_2 - \hat{a}_3)}{2} - 1 \right) (|1\rangle_2 - \lambda |0\rangle_2) (|1\rangle_3 + \lambda |0\rangle_3) \\ &= \cos^2 \theta (\sin^2 \theta)^{\lambda^2} \left(\frac{(\hat{a}_2^\dagger + \hat{a}_3^\dagger)(\hat{a}_2 + \hat{a}_3) - 2}{8} \right) \left(-\frac{1}{\sqrt{2}} (|2\rangle_2 |0\rangle_3 + |0\rangle_2 |2\rangle_3) + 2\lambda^2 |0\rangle_2 |0\rangle_3 \right) \\ &= -\cos^2 \theta (\sin^2 \theta)^{\lambda^2} \left(\frac{\lambda^2}{2} |0\rangle_2 |0\rangle_3 + \frac{1}{4} |1\rangle_2 |1\rangle_3 \right). \end{aligned}$$

□

Remark 5. Given a state ρ_{23} , the probability of the projection \hat{F}_{23} succeeding is given by

$$\cos^4 \theta (\sin^4 \theta)^{\lambda^2} \left(\frac{\lambda^2}{2} \langle 0|_2 \langle 0|_3 + \frac{1}{4} \langle 1|_2 \langle 1|_3 \right) |\rho_{23}| \left(\frac{\lambda^2}{2} |0\rangle_2 |0\rangle_3 + \frac{1}{4} |1\rangle_2 |1\rangle_3 \right).$$

Remark 6. The projection operation \hat{F}_{23} can be expressed as a weighted normalized projection as

$$\left(\frac{-\cos^2 \theta (\sin^2 \theta)^{\lambda^2} \sqrt{1 + 4\lambda^4}}{4} \right) \left(\frac{2\lambda^2 |0\rangle_2 |0\rangle_3 + |1\rangle |1\rangle_3}{\sqrt{1 + 4\lambda^4}} \right).$$

Remark 7. For states

$$|\psi\rangle_{12} = \frac{|0\rangle_1 |0\rangle_2 + \xi |1\rangle_1 |1\rangle_2}{\sqrt{1 + \xi^2}},$$

$$|\psi\rangle_{43} = \frac{|0\rangle_4 |0\rangle_3 + \xi |1\rangle_4 |1\rangle_3}{\sqrt{1 + \xi^2}},$$

can be entanglement swapped into a state $|\psi\rangle_{14} = (|0\rangle_1 |0\rangle_4 + \xi |1\rangle_1 |1\rangle_4) / \sqrt{1 + \xi^2}$, using \hat{F}_{23} of Prop. 4 with $\lambda = \sqrt{\xi/2}$. The corresponding success probability is given by

$$\left(\frac{\xi^2}{1 + \xi^2} \right) \frac{\cos^4 \theta (\sin^2 \theta)^\xi}{16}$$
